JOURNAL OF SOLID STATE CHEMISTRY **141,** 160–163 (1998)
ARTICLE NO. SC987937

Magnetic Structure and Properties of $CsMnHP_3O_{10}$

A. J. Wright and J. P. Attfield[1]

Department of Chemistry, University of Cambridge, Lensfield Road, Cambridge CB2 1EW, United Kingdom

Received March 19, 1998; in revised form June 8, 1998; accepted June 23, 1998

Through the use of magnetic susceptibility and low-temperature neutron powder diffraction techniques, $CsMnHP_3O_{10}$ has been found to behave as a Curie–Weiss paramagnet at high temperatures and to order antiferromagnetically below a Néel temperature of 11 K. The magnetic structure is commensurate with the nuclear cell doubled in the *c* direction, giving a magnetic cell of $a = 8.9384(6)$ Å, $b = 8.6385(6)$ Å, $c = 12.9991(9)$ Å, $\beta = 113.472(2)^\circ$, and $Z = 4$. $CsMnHP_3O_{10}$ has a collinear antiferromagnetic structure with magnetic symmetry group C2′ and Mn^{3+} spins lying in the *ac* plane. © 1998 Academic Press

INTRODUCTION

Inorganic framework materials have important and varied chemical properties, placing them at the forefront of current research. With the ability to catalyze organic reactions within their frameworks (1), to exhibit enhanced ion exchange properties or high ionic conductivity (2, 3), these materials can find applications in many areas such as catalysis, rechargeable batteries and fuel cell research. These properties can be attributed to the open framework structures adopted by these materials and have led to an intensive worldwide search for materials with similar structural characteristics. Among the numerous new examples are transition metal phosphate frameworks such as FePO's (4), ZnPO's (5) and CoPO's (6). The magnetic properties of many of these materials are also of fundamental interest in understanding the nature of magnetic interactions.

We are currently searching for new framework materials with the ability to "switch" between distinct framework geometries by means of ion exchange, leading to the possibility of flexible host materials. This behavior, first demonstrated by Li^+/H^+ exchange in $MnAsO_4 \cdot H_2O$ (7), requires the presence of Jahn–Teller cations in the framework. The exchange of Li^+ for H^+ produces a switch in the framework geometry, resulting from cooperative changes to the Jahn–Teller distortions of the MnO_6 octahedra. In the magnetic structure this causes a switch from antiferromagnetic to ferromagnetic superexchange interactions within the chains of MnO_6 octahedra, although the material remains an antiferromagnet overall (8). These interesting properties have led us to study the series of phases $AMnHP_3O_{10}$ (A = K, Rb, Cs), which also contain high-spin $3d^4$ Mn^{3+}. The structure of $CsMnHP_3O_{10}$ has previously been reported (9) from a single-crystal X-ray diffraction study and consists of chains of HP_3O_{10} units, interlinked by tetragonally distorted MnO_6 octahedra, to form a three-dimensional framework. Recently, we have reported the structure and magnetic properties of $RbMnHP_3O_{10}$ (10), which has the same manganese triphosphate framework as $CsMnHP_3O_{10}$ but a doubled structural unit cell due to a different A cation coordination. These can be contrasted to other $M^{I}M^{III}HP_3O_{10}$ materials, such as $NH_4AlHP_3O_{10}$ (11) and $CsGaHP_3O_{10}$ (12), which have the M^{I} cations separating layers of $HP_3O_{10}^{4-}$ and $M^{III}O_6$ units. Here we report the low-temperature crystal structure and magnetic properties of $CsMnHP_3O_{10}$ and some attempts to exchange the H^+ ion by Li^+.

EXPERIMENTAL

$CsMnHP_3O_{10}$ was prepared from a solution of Cs_2CO_3, Mn_2O_3, H_3PO_4 (85%), and concentrated HNO_3 in a molar ratio of $Cs:Mn:P:N = 9:2:30:10$. This solution was heated to 250°C for 48 h and then slow cooled to room temperature over 12 h, after which the violet microcrystalline product was collected by filtration and washed with water. The nitric acid in the reaction mixture maintains the Mn^{3+} oxidation state during the reaction.

Initial characterization of the polycrystalline product using X-ray powder diffraction showed it to be $CsMnHP_3O_{10}$ (9). Neutron powder diffraction data were collected at 2 K, with a wavelength of 2.4177 Å, for 40 min on the D20 instrument at ILL, Grenoble. This instrument contains 1600 detectors positioned in 0.1° intervals in the range 0–160° 2θ. Rietveld analyses (13) of these data were performed using the GSAS software package (14) to refine the crystal and magnetic structures.

[1]To whom correspondence should be addressed. E-mail: jpa14@cam.ac.uk.

0022-4596/98 $25.00

Magnetic susceptibility data were collected on a 57.9 mg sample of $CsMnHP_3O_{10}$ from 4–100 K in a field of 1 T on a Quantum Design SQUID magnetometer. The sample had previously been cooled in zero field.

Ion exchange of H^+ for Li^+ was attempted using a number of methods. These included a solid-state reaction of intimately mixed $CsMnHP_3O_{10}$ and a lithium salt ($LiNO_3$, Li_2CO_3, LiOH, or LiCl) in molar ratios varying from 1 : 1 to 1 : 10 at temperatures ranging from 150 to 250°C for up to 4 weeks. In those cases when a reaction occurred, a mixture of phases was formed including Li_3PO_4, which indicated that the framework structure had been broken down. No evidence for a Li-exchanged product was observed.

RESULTS

The magnetic susceptibility data (Fig. 1) show that $CsMnHP_3O_{10}$ orders antiferromagnetically with $T_N = 11$ K. At higher temperatures it behaves as a Curie–Weiss paramagnet. The fitted Curie–Weiss curve (after diamagnetic correction) for $CsMnHP_3O_{10}$ gives a Weiss constant $\theta = 2.0$ K and an effective magnetic moment $\mu_{eff} = 4.9\ \mu_B$ as expected for high-spin $3d^4$ Mn^{3+}.

The Rietveld analysis of the neutron diffraction data, achieved with an asymmetry-corrected pseudo-Voigt peak shape (15, 16) and a linear interpolated background function, indicates that the previously reported room temperature $CsMnHP_3O_{10}$ structure (9) is adopted at 2 K. The final refined parameters for $CsMnHP_3O_{10}$ obtained from a fit to the nuclear and magnetic intensities (described later) are included in Table 1 and the profiles are shown in Figs. 2 and 3.

After fitting the nuclear contribution for the 2 K neutron diffraction pattern, several magnetic peaks were evident (see Fig. 3) and were indexed on an $a \times b \times 2c$ cell, relative to the nuclear unit cell parameters. The reflection conditions are consistent with magnetic symmetry group $C2'$. The magnetic intensities were Rietveld-fitted using a calculated form factor (17) and the moments of 3.98(6) μ_B were found to lie in the ac plane, 94(1)° from a and 19° from c. The relative directions of the four Mn spins in the magnetic unit cell are $(0, y, 0) +$ $(\frac{1}{2}, y + \frac{1}{2}, 0) +$, $(0, y, \frac{1}{2})-$, and $(\frac{1}{2}, y + \frac{1}{2}, \frac{1}{2})-$, as shown in Fig. 4.

TABLE 1

Refined Structural Parameters for $CsMnHP_3O_{10}$ Obtained from Rietveld Analysis of 2 K Neutron Powder Diffraction Data in Space Group $C2$, with ESD's in Parentheses

Fitting factors: $R_{wp} = 2.4\%$ $R_p = 1.7\%$ R_F (nuclear) = 3.3%
R_F(magnetic) = 13.0% $\chi^2 = 5.2$
Lattice parameters: $a = 8.9384(6)$ Å $b = 8.6385(6)$ Å $c = 6.4996(4)$ Å
$\beta = 113.477(2)°$

Atom	Site	x	y	z	U_{iso}(Å^2)[a]
Cs	2b	0	0	$\frac{1}{2}$	0.004(3)
Mn	2a	0	0.6677(14)	0	0.010(2)
P(1)	4c	0.1810(10)	0.3879(12)	0.8925(13)	0.010
P(2)	2b	0	0.5648(16)	$\frac{1}{2}$	0.010
H	2a	0	0.2561(16)	0	0.010
O(1)	4c	0.3548(10)	0.3395(12)	0.9817(11)	0.008(1)
O(2)	4c	0.1609(9)	0.5155(13)	0.0428(12)	0.008
O(3)	4c	0.1442(7)	0.4563(12)	0.6478(11)	0.008
O(4)	4c	0.0523(9)	0.2605(12)	0.8585(12)	0.008
O(5)	4c	0.9426(7)	0.6676(12)	0.6439(12)	0.008

[a] Values shown without esds were constrained to be equal to those of the atom above.

DISCUSSION

The bond distances (Table 2) show that the MnO_6 and PO_4 polyhedra are highly distorted. The MnO_6 octahedra

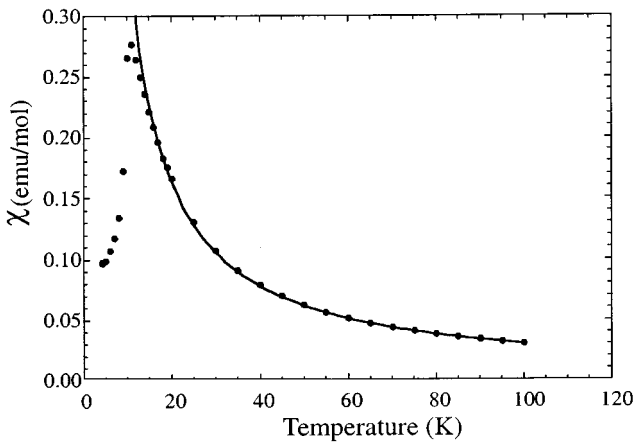

FIG. 1. Magnetic susceptibility data for $CsMnHP_3O_{10}$ between 4 and 100 K. The fitted Curie–Weiss curve is also shown.

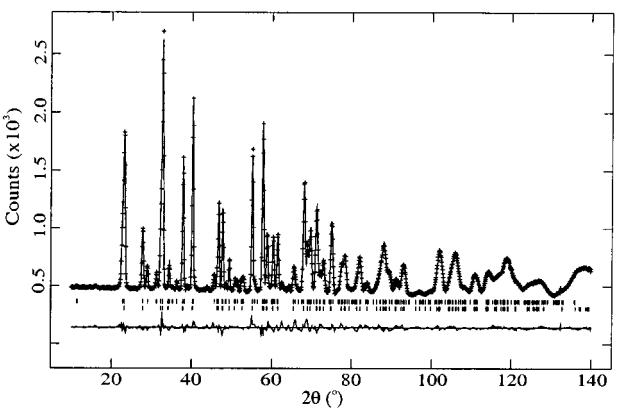

FIG. 2. Observed (+), calculated, and difference neutron powder diffraction profiles of $CsMnHP_3O_{10}$ at 2 K (upper markers for magnetic reflections, lower for nuclear).

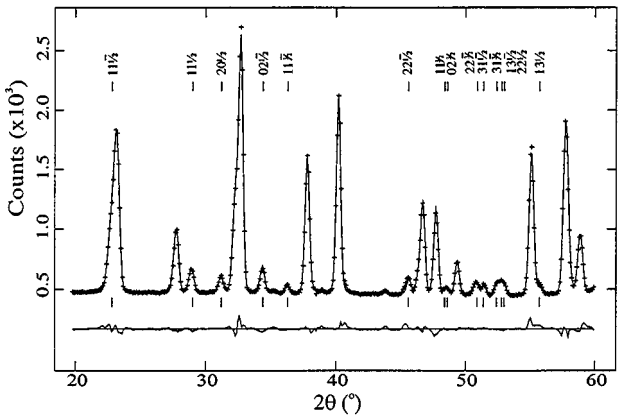

FIG. 3. Observed (+), calculated, and difference neutron powder diffraction profiles of $CsMnHP_3O_{10}$ at 2 K with magnetic peaks marked.

show a [2 + 2 + 2] Jahn–Teller distortion, with two short ($2 \times 1.885(12)$ Å), two intermediate ($2 \times 1.944(13)$ Å), and two long Mn–O bonds ($2 \times 2.162(7)$ Å). In contrast, the room temperature study (9) reported a [4 + 2] distortion ($2 \times 1.915(5)$ Å, $2 \times 1.916(5)$ Å, $2 \times 2.164(4)$ Å). This shows that an unusual crossover in the Jahn–Teller distortion mode takes place as a function of temperature. The triphosphate group contains three distorted PO_4 tetrahedra, with long P–O bonds to the bridging O(3) atom, intermediate P(1)–O(4)H distances, and short bonds to the terminal O(1), O(2), and O(5) atoms. This pattern of P–O bond lengths is typical for triphosphates and is also observed in $RbMnHP_3O_{10}$ (10). The Cs^+ is in a 10-fold coordination bonded twice to all oxygen sites. This can be contrasted to the Rb^+ coordination in $RbMnHP_3O_{10}$ (10) in which the Rb^+ is also in 10-fold coordination but bonds to only four of the five distinct oxygen sites. The size difference between Cs^+ and Rb^+ leads to the different structural symmetries of their $AMnHP_3O_{10}$ phases (Fig. 4).

TABLE 2

Bond Lengths (Å) and Selected Angles (Deg) for $CsMnHP_3O_{10}$ Obtained from Rietveld Analysis of 2 K Neutron Powder Diffraction Data, with ESDs in Parentheses

Mn–O(1)	1.944(13) [×2]	O(1)–Mn–O(1′)	80.4(6)
Mn–O(2)	1.885(12) [×2]	O(1)–Mn–O(2)	173.1(6)
Mn–O(5)	2.162(7) [×2]	O(1)–Mn–O(2′)	94.1(3)
		O(1)–Mn–O(5)	93.8(4)
P(1)–O(1)	1.485(8)	O(1)–Mn–O(5′)	86.2(4)
P(1)–O(2)	1.531(7)	O(2)–Mn–O(2′)	91.6(8)
P(1)–O(3)	1.600(8)	O(2)–Mn–O(5)	90.0(4)
P(1)–O(4)	1.543(7)	O(5)–Mn–O(5′)	180
P(2)–O(3)	1.563(7) [×2]		
P(2)–O(5)	1.520(8) [×2]	O(1)–P(1)–O(2)	108.9(5)
		O(1)–P(1)–O(3)	105.7(6)
Cs–O(1)	3.387(8) [×2]	O(2)–P(1)–O(3)	109.5(5)
Cs–O(2)	3.295(8) [×2]	O(3)–P(2)–O(3′)	106.3(8)
Cs–O(3)	3.707(5) [×2]	O(3)–P(2)–O(5)	109.7(3)
Cs–O(4)	3.137(10) [×2]	O(3)–P(2)–O(5′)	111.3(4)
Cs–O(5)	3.125(10) [×2]	O(5)–P(2)–O(5′)	108.5(10)
H–O(4)	1.187(6) [×2]	O(4)–H–O(4’)	176.3(11)
O(4) ··· O(4′)	2.372(12)		

Strong, symmetric O(4) ··· H ··· O(4) hydrogen bonds link the triphosphate anions into chains (Fig. 5). Such bonding is found in many hydrogen phosphates (18); for example, $CaHPO_4$ has symmetric O ··· H ··· O hydrogen bonding at room temperature (19) but ordered O–H ··· O bonds at 145 K (20). However, in this study it has not been possible to detect any such H ordering at low temperatures due to the low resolution of the neutron data. To explain the lack of ion exchange, we conclude that the strong hydrogen bonding plays such a significant role in the framework that attempts to replace the H^+ lead to a breakdown of the structure, which prevents this material from acting as a switchable framework.

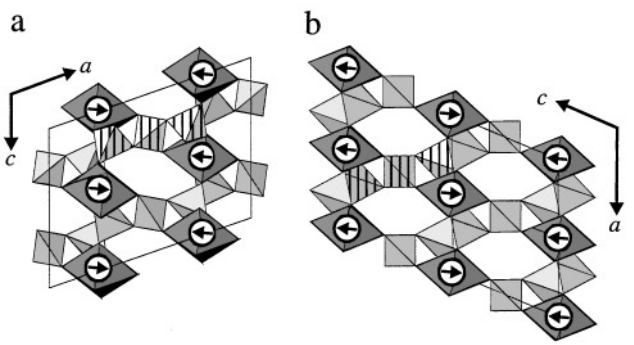

FIG. 4. [010] projection of the nuclear and magnetic structures of (a) $RbMnHP_3O_{10}$ and (b) $CsMnHP_3O_{10}$ showing the nuclear unit cell. Only the MnO_6 and PO_4 polyhedra are shown and a single P_3O_{10} unit is hatched in each case.

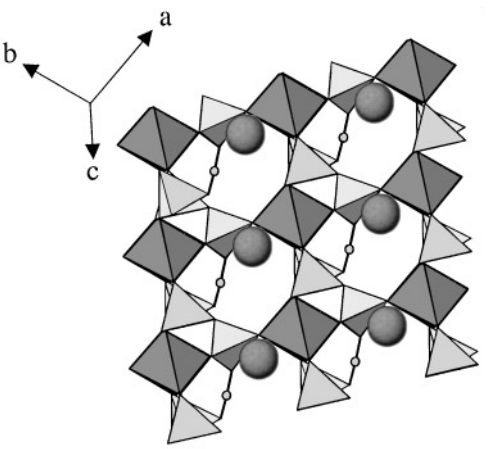

FIG. 5. A polyhedral view of the structure of $CsMnHP_3O_{10}$ showing Cs (large spheres) and H atoms (small spheres) enclosed in channels. The symmetric O(4)–H–O(4′) hydrogen bonds are also displayed.

The sharp Néel transition observed in the susceptibility data collected from $CsMnHP_3O_{10}$ indicate that three-dimensional antiferromagnetic order occurs below 11 K, and the magnetic structure obtained from the low-temperature neutron data is in accordance with this. The magnetic superexchange interactions between spins are mediated by Mn–O–P–O–Mn linkages. Each Mn spin is connected to six others: four in the *ab* plane via Mn–O(1)–P(1)–O(2)–Mn′ bridges, which are apparently ferromagnetic, and two in the *c* direction through antiferromagnetic Mn–O(5)–P(2)–O(5′)–Mn′ linkages. Overall, this corresponds to a primitive tetragonal interaction network giving rise to nonfrustrated antiferromagnetic order. The refined magnetic moment of 3.98(6) μ_B is close to the theoretical value of 4 μ_B, although a reduction due to covalency is usually found and this value seems anomalously high for reasons that are not clear. (The moment was not changed significantly by refining an absorption correction to the data.) The moments lie in the *ac* plane (Fig. 4), 6° from the direction of the long Mn–O(5) bonds (these bonds are 100° from *a* and 13° from *c*), showing that the easy axis is determined by the local electronic anisotropy of the Jahn–Teller distorted MnO_6 octahedra.

$RbMnHP_3O_{10}$ and $CsMnHP_3O_{10}$ have the same $MnHP_3O_{10}^-$ framework although the different cation coordinations lead to different structural unit cells. $RbMnHP_3O_{10}$ has $C2/c$ symmetry whereas $CsMnHP_3O_{10}$ has C2 symmetry, and the cell vectors are related by $\mathbf{a}_{Rb} = \mathbf{a}_{Cs} + \mathbf{c}_{Cs}$, $\mathbf{b}_{Rb} = \mathbf{b}_{Cs}$, $\mathbf{c}_{Rb} = \mathbf{a}_{Cs}$. Despite these differences their magnetic structures are identical (Fig. 4) as these depend only on the framework topology and the local anisotropy of the MnO_6 octahedra.

ACKNOWLEDGMENTS

We thank Dr. P. Radaelli for assistance in the collection of neutron data and EPSRC for provision of neutron facilities and Grant GR/K75040. Magnetic susceptibility measurements were made at the Cambridge IRC in Superconductivity.

REFERENCES

1. J. M. Thomas, *Angew. Chem., Int. Ed. Engl.* **33,** 913 (1994).
2. R. Brochu, A. Lamzibri, A. Aadane, S. Arsalane, and M. Ziyad, *Eur. J. Solid State Inorg. Chem.* **28**, 253 (1991).
3. A. Clearfield, *Eur. J. Solid State Inorg. Chem.* **28,** 37 (1991).
4. D. R. Corbin, J. F. Whitney, W. C. Fultz, G. D. Stucky, M. M. Eddy, and A. K. Cheetham, *Inorg. Chem.* **25,** 2279 (1986).
5. W. T. A. Harrison, T. M. Nenoff, M. M. Eddy, T. E. Martin, and G. D. Stucky, *J. Mater. Chem.* **2,** 1127 (1992).
6. J. Chen, R. H. Jones, S. Natarajan, M. B. Hursthouse, and J. M. Thomas, *Angew. Chem., Int. Ed. Engl.*, **33,** 639 (1994).
7. M. A. G. Aranda, J. P. Attfield, and S. Bruque, *J. Chem. Soc., Chem. Commun.* 604 (1991).
8. M. A. G. Aranda, J. P. Attfield, S. Bruque, and R. B. Von Dreele, *J. Chem. Soc., Chem. Commun.* 155 (1994).
9. E. V. Murashova, and N. N. Chudinova, *Kristallografiya* **40,** 476 (1995).
10. A. J. Wright, and J. P. Attfield, *Inorg. Chem.* **37,** 3858 (1998).
11. M. T. Averbuch-Pouchot, A. Durif, and J. C. Guitel, *Acta Crystallogr., Sect. B* **33,** 1436 (1977).
12. N. Anisimova, M. Bork, R. Hoppe, and M. Meisel, *Z. Anorg. Allg. Chem.*, **621,** 1069 (1995).
13. H. M. Rietveld, *J. Appl. Crystallogr.* **2,** 65 (1969).
14. A. C. Larson, and R. B. Von Dreele, Los Alamos National Laboratory Report No. LA-UR-86-748, 1994.
15. P. Thompson, D. E. Cox, and J. B. Hastings, *J. Appl. Crystallogr.*, **20,** 79 (1987).
16. C. J. Howard, *J. Appl. Crystallogr.* **15,** 615 (1982).
17. P. J. Brown, in "International Tables for Crystallography" (T. Hahn, Ed.), Vol. C, pp. 391, Kluwer Academic Publishers, Dordrecht, 1992.
18. J. Emsley, *Chem. Soc. Rev.* **9,** 91 (1980).
19. M. Catti, G. Ferraris, and A. Filhol, *Acta Crystallogr., Sect. B* **33,** 1223 (1977).
20. M. Catti, G. Ferraris, and S. A. Mason, *Acta Crystallogr., Sect. B* **36,** 254 (1980).